NUMERICAL SIMULATION OF MIXING IN AN INLET-FUELED HYPERSONIC AIR-BREATHING PROPULSION

Jae Won Kim, Oh Joon Kwon
Department of Aerospace Engineering, Korea Advanced Institute of Science and Technology 291, Daehak-ro, Yuseong-gu, Daejeon 34141, Republic of Korea.
jwkim1225@kaist.ac.kr

Keywords: *inlet injection, hypersonic flow, computational fluid dynamics*

Abstract

In the present study, injection of the gaseous hydrocarbon fuels in the inlet of a scramjet engine has been numerically investigated by using a non-equilibrium flow solver based on unstructured meshes. A generic two-dimensional four-shock inlet configuration, which was designed to fly at an altitude of 22 km with a flight Mach number of 6, was adopted, and under-expanded ethylene fuels were injected from three orifice injectors at the end of the first ramp. To investigate the effect of fuel injection angle, equivalent ratio, and inlet ramp angle on the mixing efficiency, the calculations were made by varying one parameter at each calculation while the other two are held constant. It was found that the overall fuel-air mixing efficiency increases as the fuel injection angle and equivalent ratio decrease, and inlet ramp angle increases due to the changed shock structures in the inlet internal region.

1 Introduction

One of the key technologies required for hypersonic scramjet engines is to achieve efficient fuel-air mixing and combustion heat release during the extremely short residence time of the air inside the supersonic combustor. Up until recently, quite a few different injection techniques have been developed to enhance the supersonic fuel-air mixing [1]. One of the techniques is relocating the fuel injectors from the traditional combustor positions to the inlet [2-5]. Since fuel-air mixing occurs in the inlet before the fuel reaches the combustion chamber, this approach has an advantage of significantly increasing the mixing length of fuel-air. Inlet injection also has a potential of reducing the length of the combustion chamber required to contain the complete combustion reaction. Since the surface heat flux and the skin friction drag are at their peaks in the combustion chamber, this length reduction could increase net engine thrust.

Previous studies about the inlet injection have been mostly focused on the Mach numbers of 8 and above. Recently, to develop hydrocarbon-fueled scramjet engines typically operating between the Mach numbers of 4 and 8, there has been has renewed interests about the inlet injection. The conventional fuel-injection methodology may not be as effective for hydrocarbon fuels because of its slow kinetic rates, ignition delay times, and the short residence time in the combustor [2].

Several studies have been conducted to investigate the possibility and the effectiveness of the injection of gaseous hydrocarbon fuels in the inlet-fueled scramjet engines. Guoskov et al. [4] performed a numerical investigation of the normal injection of gaseous hydrocarbon fuel in an air inlet from the wall injectors located behind thin swept pylons at Mach numbers of 6 and 8. Mixing in the near vicinity of the pylons was calculated by using the Favre-averaged Navier-Stokes equations for three-dimensional, turbulent, multispecies, nonreacting flows. For the fuel-air equivalence ratios between 0.3 and 0.7, the fuel-air mixing efficiencies between 0.95 and 0.98 was reported before exiting an inlet channel with a length of 0.65 m. Wang et al. [5] conducted a numerical simulation of gaseous hydrocarbon fuel injected quasi parallel to the compression surface of the inlet via a cantilevered ramp injector. For the methane-fueled inlet, fuel-air mixing efficiencies in the range of 75.5-95.8% were presented at a low risk of premature ignition. The effects of inlet compression, the fuel-injection conditions, fuel selection and properties, and injector geometry on the overall fuel-air mixing efficiency and the attendant flow losses at the exit of inlet were also investigated in detail.

In the present study, injection of the gaseous hydrocarbon fuels in the inlet of a scramjet engine has been numerically investigated by using a compressible Navier-Stokes flow solver including a non-equilibrium model on unstructured meshes. For this purpose, a generic two-dimensional inlet configuration consisting of four straight ramps of equal turning angles was adopted, and ethylene fuels were injected from three orifice injectors at the end of the first ramp. To investigate the effect of fuel injection angle, equivalent ratio, and inlet ramp angle on the overall fuel-air mixing characteristics, the parametric study was conducted. Particular attention was given to the mixing of fuel-air, which is difficult or impossible to measure experimentally.

2 Numerical Method

2.1 Numerical Scheme

The compressible Navier-Stokes equations were discretized by using a vertex-centered finite-volume method based on unstructured meshes. The flow domain was divided into a finite number of control volumes surrounding each vertex, which were made of non-overlapping median-dual cells whose boundary surfaces were defined by the cell centroid, face centroid and the midpoint of the edge of the unstructured mesh. The inviscid flux terms were approximated using AUSMPW+ scheme [6], whereas the viscous flux terms were evaluated by adopting a modified central difference method [7]. To achieve second-order spatial accuracy, the flow variables at each dual face were assessed by applying a least-square reconstruction technique [8]. An implicit time integration method based on a linearized second-order Euler backward differencing was applied to advance the solution in time. The linear system of equations was solved at each time step by using a point Gauss-Seidel iteration method. To enhance the convergence, a local time stepping procedure was adopted. A parallel algorithm based on a domain decomposition strategy was adopted to reduce the large computational time involved in the three-dimensional flow calculations. To estimate the turbulent eddy viscosity, the k-ω SST turbulence model was adopted. These additional equations were solved separately from the flow equations in a loosely coupled manner.

2.2 Thermochemistry

The pressure of the mixture was obtained by using Dalton’s law of partial pressures with the assumption of perfect gas behavior for each species. The transport properties were calculated from the curve fits utilized by Gordon and McBride [9] in the NASA Chemical Equilibrium with Applications (CEA) program. For calculating the mixture transport properties, Wilke’s semi-empirical mixing rule [10] was adopted. The heat fluxes were modeled using Fourier’s law. Also, the diffusive flux of each species was modeled using Fick’s law which was modified to enforce that sum of the diffusion fluxes is zero [11].

2.3 Validation

For the validation of the present flow solver, the transverse gas injection across a supersonic flow was simulated. The two-dimensional injection experiments by Spaid and Zukoski [12] were considered as the test cases. In the experiment, sonic jet of nitrogen was vertically injected into freestream at a Mach number of 3.5 through a slot of width 0.2667 mm located at 228.6 mm behind the leading edge. In the present calculation, the same computation domain to that of Chenault and Beran [13] was constructed for a direct comparison. The unstructured hybrid

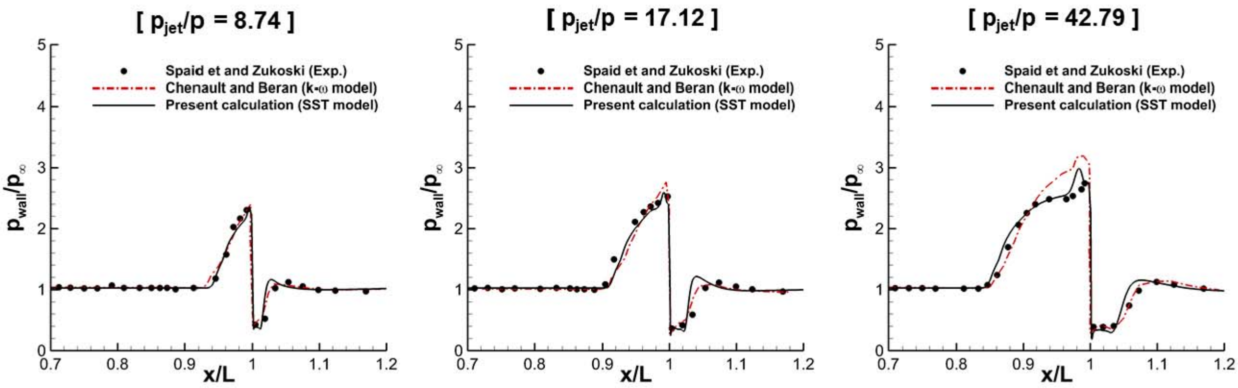

Fig. 1. Comparison of Surface Static Pressure Distributions for Spaid and Zukoski's Configuration [12].

mesh consisted of 99,715 cells and 62,065 nodes.

In Fig. 1, the calculated surface static pressure distributions are compared with the experimental date of Spaid and Zukoski and other numerical predictions of Chenault and Beran for pressure ratios ranging from 8.74 to 17.12. In the present calculations, the k-ω SST turbulence model was used. It is shown that, at lower pressure ratios, both predictions with different turbulence models are in relatively good agreements with the experimental data. As the pressure ratio increases, difference between the numerical results and the experimental data becomes more significant. At the upstream of the injector, both predictions with the k-ω model and SST models matches well the experimental pressure distributions. However, the SST model by the present calculations predicts the peak pressure values closer to the experimental data than those of the k-ω model by Chenault and Beran. At the downstream of the injector, the predicted pressure distributions by the k-ω model are in slightly better agreement with the experiment than those of the SST model.

3 Results and Discussion

In the present study, a generic two-dimensional supersonic inlet consisting of four straight ramps of equal turning angles was simulated at an altitude of 22 km with a free-stream Mach number of 6. The inlet consists of four ramps with a ramp angle of 12.4 deg. This configuration was designed such that the flow turns by the same angle as the inlet ramp angle, and that the flow reaches a Mach number of 1.8 at the inlet exit. Figure 2 shows the two-dimensional shock pattern and three-dimensional geometry of the inlet. The figure clearly indicates the formation of oblique shock waves, and confirms that the inlet geometry is designed such that the first two oblique shock waves from the first and second ramps meet at the leading edge of the cowl. For all calculation cases, the inlet was assumed to operate at the design condition. An under-expanded ethylene (C_2H_4), a surrogate test fuel for hydrocarbon scramjet, was considered in the present calculations. Three fuel orifice injectors 2 mm in diameter were located at the end of the first ramp. The fuel was injected from the inlet injectors at the sonic conditions.

To examine the flow behavior and the inlet performance, three parameters, the angle of injected fuel θ_{inj} , the equivalence ratio of fuel-air mixture Φ , and the angle of inlet ramp θ_{inlet} ,

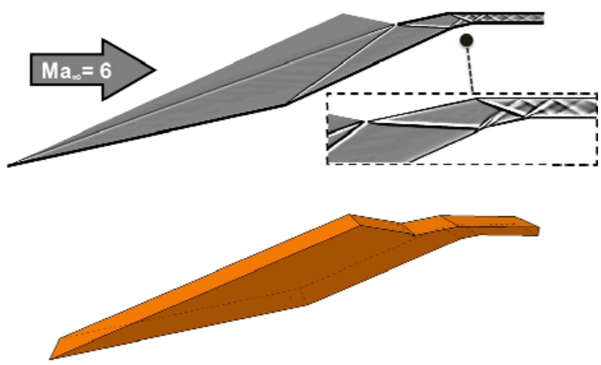

Fig. 2. Two-dimensional Shock Pattern (top) and Three-dimensional Geometry (bottom) of Inlet.

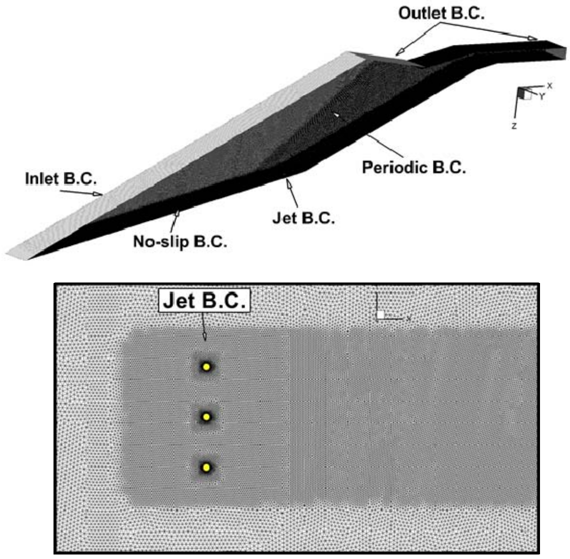

Fig. 3. Computational Domain and Boundary Conditions.

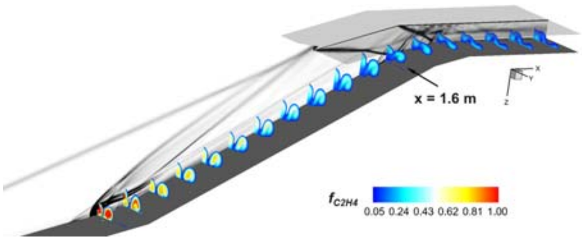

Fig. 4. Density Gradient Magnitude Contours at Mid x-z Plane and Ethylene Mass Fraction Contours at Several Cross-sectional y-z planes.

were chosen. To test the effects of the three parameters, the simulations were performed by varying one parameter at each calculation while the other two are held constant.

In Fig. 3, the computational domain and the boundary conditions applied are presented. The internal inlet walls were assumed to be no-slip adiabatic surfaces. A periodic condition was imposed at the side boundaries. The supersonic inflow and jet exit flow conditions were specified at the upstream and jet boundaries, respectively. The exiting plane was set to the zeroth-order supersonic outflow condition. The hybrid unstructured mesh contains 6,368,858 prismatic cells and 20,979,257 tetrahedral cells, and the number of nodes is 6,931,836.

In Fig. 4, the density gradient magnitude contours and the fuel mass fraction contours are presented at the mid x-z plane and several cross-sectional y-z planes, respectively. It is shown that the jet expands rapidly and penetrates the boundary layer, developing a system of shock and recirculation regions fore and aft of the injector exit. At the upstream of the injector, a jet-induced bow shock originating from the blocked crossflow merges with the oblique shock wave from the first ramp. The shock structures impinging and reflecting on the inlet internal walls are also observed at the downstream of the inlet, which contributes toward the supersonic fuel-air mixing enhancement.

To quantify the mixing performance of the inlet, the mixing efficiency was calculated. The mixing efficiency is defined as the ratio of the fuel mass flow rate that is mixed with air and reacts to the fuel mass flow rate injected through the injectors:

$$\eta_{mix}(x) = \frac{\int f_R \rho u dA}{\dot{m}_{fuel}} \quad (1)$$

$$f_R = \begin{cases} f & if \ \ f \le f_{st} \\ f_{st}(1-f)/(1-f_{st}) & if \ \ f > f_{st} \end{cases} \quad (2)$$

where f and f_{st} are the mass fraction of ethylene and the stoichiometric mass fraction of ethylene, respectively. The stoichiometric mass fraction of ethylene was approximated to be 0.0638.

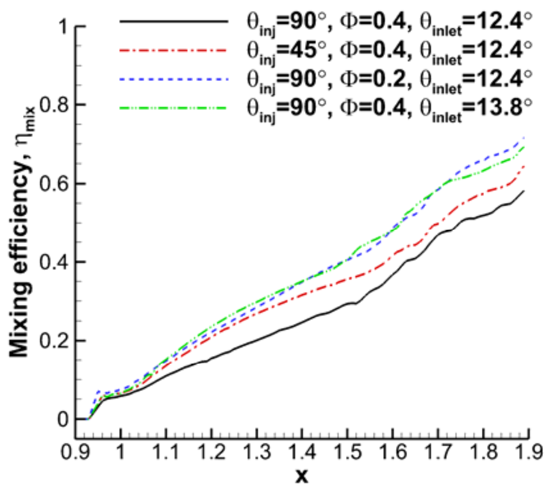

Fig. 5. Mixing Efficiency Comparison for Varying Injection Angle, Equivalence Ratio and Inlet Ramp Angle.

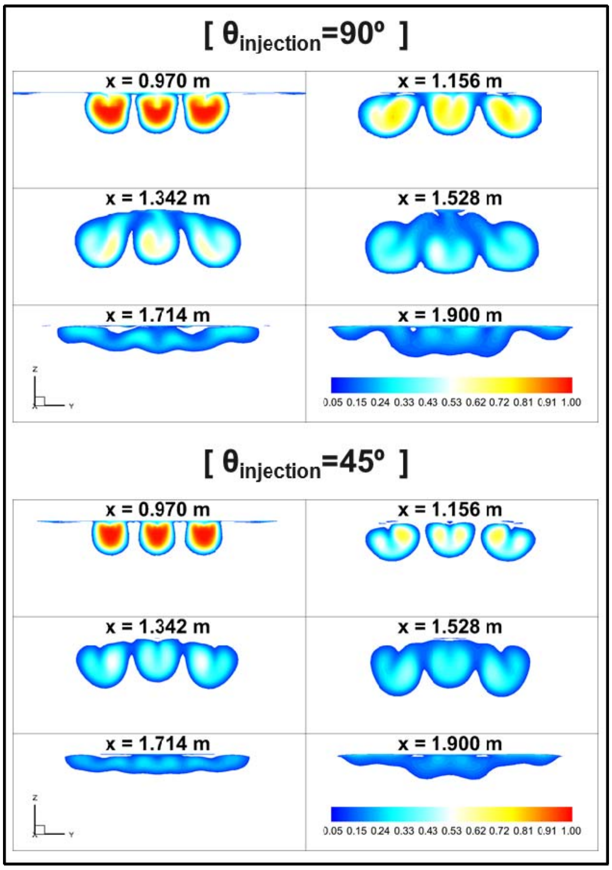

Fig. 6. Comparison of Ethylene Mass Fraction Contours between Different Injection Angles.

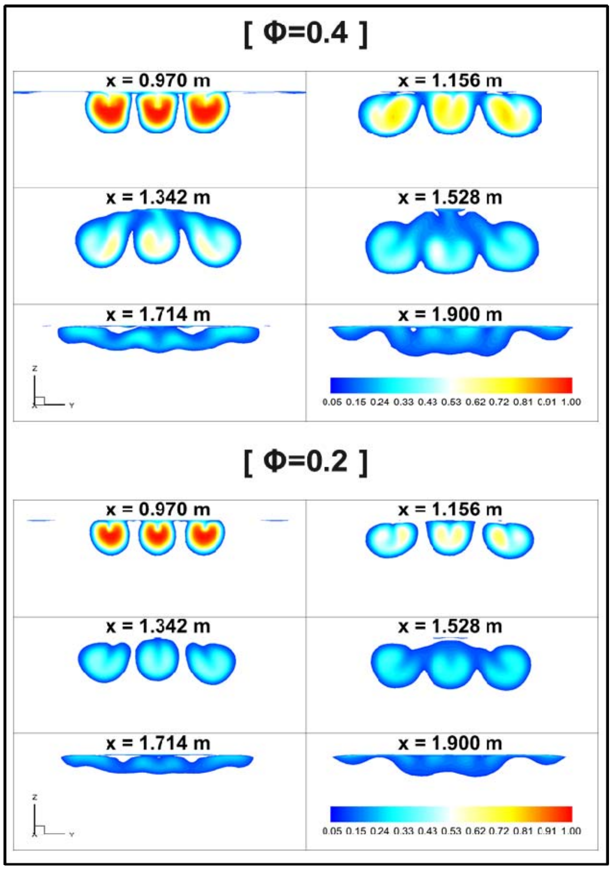

Fig. 7. Comparison of Ethylene Mass Fraction Contours between Different Equivalence Ratios.

In Fig. 5, the mixing efficiencies for different parameter variations are presented. It is observed that the efficiency increases drastically at x=1.6 m due to the shock impinging into the fuel-air interface, destroying the concentrated fuel core structure.

In Fig. 6, the ethylene mass fraction contours at several cross-sectional y-z planes are compared between the two angles of the injected fuel of 90 deg and 45 deg. It is shown that counter rotating vortex pairs, which control the fuel-air mixing process, are created behind the downstream of the injectors at x = 0.970-1.342 m. At the injection angle of 45 deg, the core region of the fuel is somewhat smaller than that of the 90 degree injection angle, leading to stronger counter rotating vortices. This is directly related to the increment of the mixing efficiency as shown in Fig. 5. When the injection angle is decreased to 45 deg, the mixing efficiency is increased by approximately 11% compared to that of the injection angle of 90 deg.

In Fig. 7, the ethylene mass fraction contours at several cross-sectional y-z planes are compared between the two equivalence ratios of the fuel-air mixture of 0.4 and 0.2. In the case of the equivalence ratio of 0.4, the jet momentum flux is higher than that of the equivalence ratio of 0.2, resulting in a deeper penetration in the z direction. As expected, the mixing efficiency increases when the equivalence ratio is decreased, as shown in Fig. 5. However, low equivalence ratio may potentially reduce the thrust of the vehicle.

In Fig. 8, the ethylene mass fraction contours at several cross-sectional y-z planes are compared between the two angles of the inlet ramp of 12.4 deg and 13.8 deg. During the initial development, the inlet compression has no impact on the fuel-air mixing. At further downstream, however, when the inlet ramp angle is increased to 13.8 deg, the lateral mixing

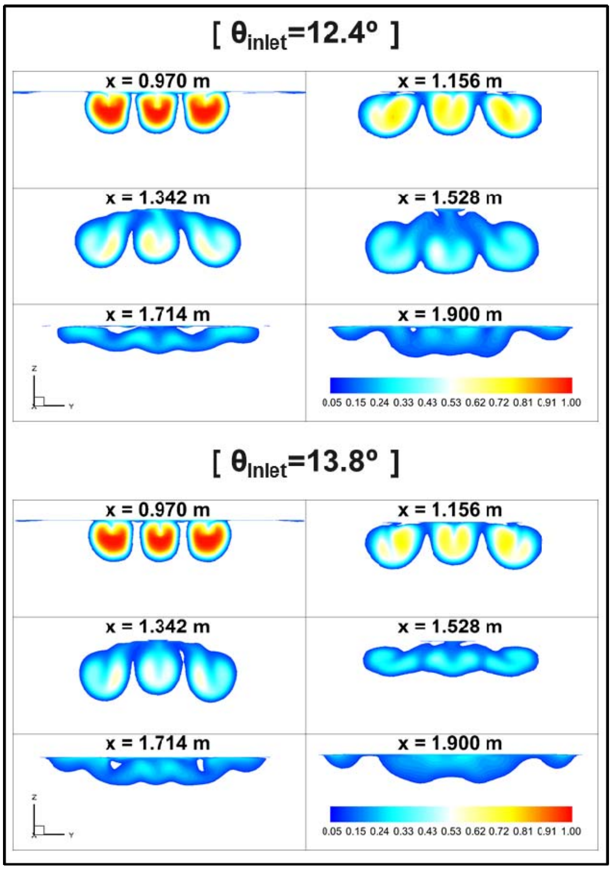

Fig. 8. Comparison of Ethylene Mass Fraction Contours between Different Inlet Ramp Angles.

at x = 1.528 m is relatively enhanced under a high pressure environment. Increasing the inlet ramp angle from 12.4 deg to 13.8 deg resulted in an 18.2% improvement in the mixing efficiency.

4 Conclusions

In the present study, numerical simulations of the inlet-fueled scramjet engine were conducted using a non-equilibrium flow solver based on unstructured meshes. A generic four-shock inlet configuration for the flight Mach number of 6 was selected, and three orifice injectors were located at the end of the first ramp. To examine the effect of fuel injection angle, equivalent ratio, and inlet ramp angle on the fuel injection performance, the parametric study was performed. The numerical results show that the shock structures impinging and reflecting on the inlet internal walls significantly influence on the mixing efficiency, breaking the fuel-air interface. At the injection angle of 45 deg, the mixing efficiency is increased by about 11% compared to that of the injection angle of 90 deg. Similarly, increasing the inlet ramp angle from 12.4 deg to 13.8 deg resulted in an 18.2% improvement in the mixing efficiency. The mixing efficiency increases when the equivalence ratio is decreased, but the low equivalence ratio may potentially reduce the thrust of the vehicle. In the future, the possibility of premature ignition of the combustible mixture inside the inlet will be assessed via a finite-rate chemical reaction model.

Acknowledgments

This work was supported by the High-Speed Air-breathing Engine Laboratory of Agency for Defense Development.

References

[1] Curran, E. Scramjet engines: the first forty years. *Journal of Propulsion and Power*, Vol. 17, No. 6, pp 1138-1148, 2001.

[2] Vinogradov, V. A, Shikhman, Y. M and Segal, C. Review of fuel pre-injection studies in a high speed airflow. *44th AIAA Aerospace Sciences Meeting and Exhibit*, Reno, NV, U.S.A., AIAA Paper 2006-1030, 2006.

[3] Turner, J. C and Smart, M. K. Application of inlet injection to a three-dimensional scramjet at Mach 8. *AIAA Journal*, Vol. 48, No. 4, pp 829-838, 2010.

[4] Guoskov, O. V, Kopchenov, V. I, Lomkov, K. E, Vinogradov, V.A and Waltrup, P. J. Numerical research of gaseous fuel preinjection in hypersonic three-dimensional inlet. *Journal of Propulsion and Power*, Vol. 17, No. 6, pp 1162-1169, 2001.

[5] Wang, Y. W and Sislian, J. P. Numerical simulation of gaseous hydrocarbon fuel injection in a hypersonic inlet. *Journal of Propulsion and Power*, Vol. 26, No. 5, pp 1114-1124, 2010.

[6] Kim, K. H and Kim, C. Accurate, efficient and monotonic numerical methods for multi-dimensional compressible flow part1: multi-dimensional higher order interpolation scheme. *Journal of Computational Physics*, Vol. 208, No. 2, pp 527-569, 2005.

[7] Mathur, S. R and Murthy, J. Y. A pressure-based method for unstructured meshes. *Numerical Heat Transfer*, Vol. 31, No. 2, pp 195-215, 1997.

[8] Barth, T. A 3-d upwind Euler solver for unstructured meshes. *10th Computational Fluid Dynamics*

Conference, Honolulu, HI, U.S.A., AIAA Paper 1991-1548, 1991.

[9] Gordon, S and McBride, B.J. Computer program for calculation of complex chemical equilibrium compositions and applications. Part 1:analysis. *NASA RP-1311*, 1994.

[10] Wilke, C. R. A viscosity equation for gas mixtures," *Journal of Chemical Physics*. Vol. 18, pp 517-519, 1950.

[11] Sutton, K and Gnoffo, P. A. Multi-component diffusion with application to computational aerothermodynamics. *7th AIAA/ASME Joint Thermophysics and Heat Transfer Conference*, Albuquerque, NM, U.S.A., AIAA Paper 1998-2575, 1998.

[12] Spaid, F. W and Zukoski, E. E. A study of the interaction of gaseous jets from transverse slots with supersonic external flows. *AIAA Journal*, Vol. 6, No. 2, pp 205-212, 1968.

[13] Chenault, C. F and Beran, P. S. K-ε and Reynolds stress turbulence model comparison for two-dimensional injection flows. *AIAA Journal*, Vol. 36, No. 8, pp 1401-1412, 1998.

Copyright Statement